IEEE Access
Multidisciplinary ⋮ Rapid Review ⋮ Open Access Journal

Received 27 March 2023, accepted 11 April 2023, date of publication 14 April 2023, date of current version 25 April 2023.

Digital Object Identifier 10.1109/ACCESS.2023.3267163

RESEARCH ARTICLE

Risk Mitigation & Profit Improvement of a Wind-Fuel Cell Hybrid System With TCSC Placement

JAYANTA BHUSAN BASU[1], SUBHOJIT DAWN[2], PRADIP KUMAR SAHA[3], MITUL RANJAN CHAKRABORTY[1], FAISAL ALSAIF[4], SAGER ALSULAMY[5], AND TAHA SELIM USTUN[6], (Member, IEEE)

[1]Siliguri Institute of Technology, Darjeeling, West Bengal 734009, India
[2]Velagapudi Ramakrishna Siddhartha Engineering College, Vijayawada, Andhra Pradesh 520007, India
[3]Jalpaiguri Government Engineering College, Jalpaiguri, West Bengal 735102, India
[4]Department of Electrical Engineering, College of Engineering, King Saud University, Riyadh 11421, Saudi Arabia
[5]Energy and Climate Change Division, Sustainable Energy Research Group, Faculty of Engineering and Physical Sciences, University of Southampton, SO16 7QF Southampton, U.K.
[6]Fukushima Renewable Energy Institute, AIST (FREA), Koriyama 963-0298, Japan

Corresponding authors: Jayanta Bhusan Basu (jbb.sit@gmail.com), Subhojit Dawn (subhojit.dawn@gmail.com), and Taha Selim Ustun (selim.ustun@aist.go.jp)

This work was supported by the Researchers Supporting Project, King Saud University, Riyadh, Saudi Arabia, under Grant RSPD2023R646.

ABSTRACT The incorporation of renewable energy into the existing electrical system is vital in a competitive electrical system. The unpredictable nature of renewable sources is the main obstacle to energy source integration. Since wind energy is unpredictable, integrating it into an existing thermal system requires some additional operating procedures to maintain the economic and functioning sustainability of the system. In a competitive power network, renewable energy uncertainty creates an imbalance cost (IC) which directly affects the system economy. This study investigates system generation costs, voltage profiles, and electric losses in a deregulated power market incorporating wind farms (WF) & fuel cells (FC). The fuel cell has been used here as a reserve generating unit to mitigate the deficit of power in the renewable incorporated system. To check the efficacy of the presented method, two locations in India are chosen at random. To assess the imbalance cost caused by the discrepancy between forecasted (FWS) and actual wind speeds (AWS), several charge rates (i.e. surplus and deficit) were established. The electrical system has been restructured, so consumers are continually looking for efficient and stable economic power which is only possible by reducing the system risk. This paper outlines a strategy for the optimal operation of a Thyristor-Controlled Series Compensator (TCSC) and fuel cell in a wind-integrated system to maximize system profit and minimize the system risk. In this work, different algorithms like Sequential Quadratic Programming (SQP), Artificial Bee Colony Algorithms (ABC), and Moth Flame Optimization Algorithms (MFO) are used to analyze the economic and functional risk of the system. Additionally, it explains how the fuel cell system is employed to offset the wind farm integration's deviation in the real-time power market. Value-at-Risk (VaR) and conditional Value-at-Risk (cVaR) have been used for risk analysis. A modified IEEE 14-bus test system is considered to validate the entire study whereas any small, large as well as hybrid systems can be considered to perform this methodology.

INDEX TERMS Deregulated system, TCSC, wind energy, fuel cell, system profit, VaR, CvaR.

The associate editor coordinating the review of this manuscript and approving it for publication was Lei Wang.

I. INTRODUCTION

Over the last few decades, deregulated power systems have replaced the previous monopoly electricity arrangements. After the energy market was deregulated, a competitive ambiance between market participants was formed, and customers benefited from this. The inclusion of renewable resources assisted the power sector's transformation from a monopoly to a competitive one. Renewable energy has a significant potential to contribute to the world's energy supply through its capacity addition, balancing supply and demand ratio, and protecting the atmosphere. Wind power generators became the most accepted choice due to their abundance, zero carbon emissions, cleanliness, and lack of greenhouse gas emissions. There are chances to create system security risks related to power system functioning (i.e. voltage stability, frequency stability, etc.) or financial risks linked with imbalance costs owing to the unpredictable nature of renewable energy sources. Additional energy sources and storage systems are desirable to balance the power supply to combat the effects of cost imbalance. Electric utilities must augment their methods to maximize power flow over existing transmission lines due to boundaries on the construction of new transmission lines. FACTS devices are the most adaptable and practical choice for regulating the flow of power across transmission lines.

Numerous issues have been obtained in this area of research, including the use of renewable resources, different storage technologies, and FACTS devices in a deregulated system. According to Woo et al. [1], capacity constraint is one of the main issues that deregulated systems face.

Due to the intrinsic variability of wind speed, the optimal contribution of wind energy within energy markets confronts significant hurdles. As a result, such units are usually forced to sign take-or-pay contracts at prices below market clearing values. Dadashi et al. [2] has shown the effect of combining wind generators with energy storage devices to deal with the issue. Reddy and Bijwe [3] presented a methodology for renewable integrated systems to maximize system security and financial gain. A bidding technique was predicted by Matevosyan and Soder [4] to reduce the deregulated wind power market's price discrepancy. A method for evaluating how unpredictable wind speed affects a electricity market was proposed in [5].

In deregulated markets, Patil et al. [6] emphasized the significance of integrating wind energy into the system economy. Gandoman et al. [7] analyzed and addressed FACTS device uses in renewable integrated smart grids. The studies in [8] and [9] provided risk reduction methods for a wind-integrated competitive electricity market through the application of FACTS technology. Among FACTS devices, TCSC can effectively rebalance the flow of power which enhances the system's transfer efficiency. To maximize social welfare, Tiwari and Sood [10] proposes an efficient, dependable, and rapid optimization technique for the placement of TACTS devices in the system. Long et al. [11] used the Cuckoo Optimization Algorithm in his study. Nagalakshmi and Kamaraj [12] has proposed the hybrid model of TCSC using the DE algorithm for improved pool load ability security. Besharat et al. [13], [14] has presented an optimal method for TCSC placement to reduce system reactive power losses and real power performance index. Duong et al. [15] created a way to achieve a secured OPF solution during regular and contingency scenarios to increase system security under normal and abnormal conditions. Sundar and Ravikumar [16] focuses on finding the best possible solution for power flow and improving system performance. Partha et al. [17] attempts to find the best power flow by incorporating stochastic wind generators with FACTS devices. Acharya and Mithulananthan [18] assesses the effect of TCSC on congestion and spot pricing. Elmitwally and Eladl [19] proposed a method to optimally distribute FACTS devices to enhance the social benefit and lower the charges paid by market participants in a deregulated scenario.

The rising usage of renewable energy has led to the installation of an energy storage system (ESS) to reduce the erratic nature of wind generation. Over a desired time horizon, the energy storage device can change the wind energy generation pattern and smooth out its volatility. An energy storage system based on fuel cells provides the separation of power conversion and energy storage operations allowing for independent optimization. Lee [20] has investigated the implications of deregulation in the electricity energy market on a variety of distributed generation technologies including fuel cells. Smith [21] and Akinyele et al. [22] evaluated the fuel cell as an energy storage system. A freestanding hybrid solar/wind/FC power generation system was created by Fathabadi [23] for the power distribution network. A PV-solar-fuel cell-based energy system was suggested by Singh et al. [24] to satisfy the electrical power requirements of a modest community center in India. Shao et al. [25] presented a combination sharing approach of fuel cells, wind turbines, battery storage units, and demand response in a microgrid to maximize the system benefits. Mariani et al. [26] has proposed a model predictive control (MPC) method to manage a fuel cell in a wind-based system. Utomo et al. [27] discovered significant reductions in operational costs and carbon emissions during times when renewable electricity generation is high.

The extensive literature reveals that research has been done on several areas of a deregulated system with the incorporations of wind energy and energy-storing technologies. But a few things are yet to be explored in this area which has been discussed together in this work. The main highlights of this work are as follows:

- This study examines systems that use wind energy in both regulated and deregulated settings.
- In a wind-integrated deregulated power environment, a method is developed to evaluate the effects on the power system because of the unpredictable nature of the wind speed.
- If the actual and forecasted wind speeds differ, once the generating companies (GENCOs) & distribution companies (DISCOs) enter into a power supply agreement

based on a wind speed estimate, the ISO may penalize or reward the GENCOs for the deficit or excess in power delivery.

- So, to lessen the negative effects of cost imbalances, GENCOs are working to close the power gap between actual and forecasted wind speeds.
- An energy storage system is the most effective way to solve this power crisis. Storage systems in a worldwide energy market can lessen power discrepancies and the burden on thermal power plants, enabling the financial return to be realized.
- For two different sites in India, the impact of the system's imbalance cost on profit is explored with the forecasted and actual wind speed over a whole day.
- In this instance, the negative effects of cost imbalances in the combination thermal-wind-fuel cell system are addressed using a fuel cell.
- SQP, ABC, and MFO are used to judge how effective the suggested method is. The proportional studies of system risk before and after the deployment of fuel cells are highlighted here using a variety of optimization techniques.
- The impact of the cost imbalance is assessed. While this research has never been done before, its originality resides in the use of a fuel cell to maximize profit while minimizing the effects of cost imbalances.
- The impact of the TCSC and fuel cell locations on the system risk profile is also established by this analysis. TCSC is the simplest form of FACTS device that has been successfully included in the system, hence advanced FACTS devices will also be successfully incorporated into the proposed system.

This work is organized as follows: section I provides the background study along with the literature and main highlights of the work. Section II describes the different mathematical formulations used to evaluate the performance of the proposed configuration. Section III establishes the objective functions associated with the constraints for optimization. Sections IV describe the proposed method for assessing system risk and societal benefit of a deregulated system. Section V combines the results obtained for the different scenarios without & with the integration of wind energy sources. Further, the study is conducted after integrating the fuel cell into the system and optimally placing the TCSC. Comparative studies on system profit & system risk assessment using ABC, MFO, and SQP algorithms were done & finally present the conclusions of the work.

II. MATHEMATICAL FORMULATION

An objective function has been presented in this paper using a fuel cell and wind farm model.

A. DATA ON WIND SPEED

For the analysis, the actual and forecasted wind speeds for two different locations in India (Siliguri and Kolkata) are recorded. The FWS data for 11th November 2022 was gathered on 10th November, while the AWS data for 11th November 2022 was collected on November 12th [28]. Data for a height of 10 meters (h_o) was acquired. In India, a wind turbine's hub height is typically 120 meters. Therefore, the wind speed at that altitude (h) is determined [29]:

$$\frac{W_h}{W_o} = \left(\frac{h}{h_o}\right)^{\alpha} \tag{1}$$

where, 'W_h' is wind velocity at height 'h,' 'W_o' is wind velocity at a height 'h_o' and 'α' are co-efficient of Hellman. The recorded wind speed as well as the estimated wind speeds are displayed in Table 1.

TABLE 1. FWS & AWS at 10 m & 120 m height (in m/s) [28].

Hour	Siliguri				Kolkata			
	Recorded wind speed at 10 m		Calculated wind speed at 120 m		Recorded wind speed at 10 m		Calculated wind speed at 120 m	
	FWS	AWS	FWS	AWS	FWS	AWS	FWS	AWS
1	2.22	2.50	3.17	3.57	2.50	1.94	3.57	2.77
2	2.22	2.50	3.17	3.57	2.50	1.94	3.57	2.77
3	2.22	2.50	3.17	3.57	2.22	2.50	3.17	3.57
4	2.22	2.22	3.17	3.17	2.22	2.50	3.17	3.57
5	2.22	2.22	3.17	3.17	2.22	1.94	3.17	2.77
6	2.22	2.22	3.17	3.17	2.22	2.50	3.17	3.57
7	1.94	2.22	2.77	3.17	2.22	2.50	3.17	3.57
8	1.94	1.94	2.77	2.77	2.50	1.94	3.57	2.77
9	1.94	1.94	2.77	2.77	2.50	2.50	3.57	3.57
10	1.94	2.22	2.77	3.17	2.78	2.50	3.96	3.57
11	2.22	2.22	3.17	3.17	3.06	1.94	4.36	2.77
12	2.22	1.94	3.17	2.77	3.33	1.94	4.75	2.77
13	2.50	2.78	3.57	3.96	3.33	1.94	4.75	2.77
14	2.50	1.94	3.57	1.98	3.33	3.06	4.75	4.36
15	2.50	1.94	3.57	2.77	3.33	3.06	4.75	4.36
16	2.50	2.22	3.57	3.17	3.33	3.61	4.75	5.15
17	2.22	2.50	3.17	3.57	3.33	4.44	4.75	6.34
18	1.94	2.50	2.77	3.57	3.06	2.50	4.36	3.57
19	2.22	2.78	3.17	3.96	3.06	2.50	4.36	3.57
20	2.22	2.22	3.17	3.17	2.78	3.06	3.96	4.36
21	2.22	1.94	3.17	2.77	2.50	2.50	3.57	3.57
22	2.22	1.94	3.17	2.77	2.50	2.78	3.57	3.96
23	2.22	1.94	3.17	2.77	2.22	2.78	3.17	3.96
24	2.22	2.22	3.17	3.17	2.22	2.78	3.17	3.96

B. WIND POWER AND GENERATION COST ESTIMATION

The power available from a wind turbine is given by [30]:

$$P_w = \frac{1}{2}\rho a \eta v^3 \tag{2}$$

where a is the sweep-up area of the wind turbine, v is wind velocity, ρ is the density of air, η is the efficiency of the turbine. For this work, $\rho = 1.225\ kg/m^3$, the turbine rotor radius is 40 m &$\eta = 0.49$. According to Table 1, the database offers a range of wind speeds in the select cities between 1.94 and 4.44 m/s. For the wind speeds mentioned above,

TABLE 2. Calculated wind power cost for different wind velocity.

Wind velocity at 10 m height (m/sec)	Wind velocity at 120 m height (m/sec)	Power generated with 50 wind turbines (MW)	Wind power cost ($/hr)
1.94	2.77	1.61	6.032
2.22	3.17	2.40	9.004
2.50	3.57	3.42	12.820
2.78	3.96	4.69	17.586
3.06	4.36	6.24	23.407
3.33	4.75	8.10	30.389
3.61	5.15	10.30	38.637
4.44	6.34	19.21	72.033

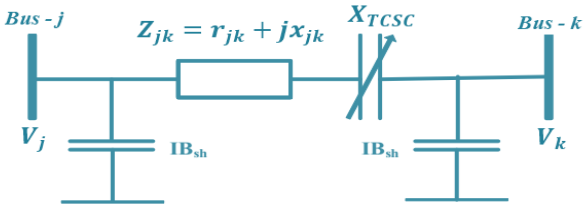

FIGURE 1. Static model of TCSC.

Table 2 shows the amount of power produced and the cost of wind energy. The cost of investment for wind energy is considered as 3.75 $/MWh [31]. The wind farm has 50 wind turbines that are all running in parallel.

C. STATIC MODEL OF TCSC

The thyristors' firing angle can change the inductor reactance, which can alter the effective impedance of the TCSC [32]. It also lowers the line's transfer reactance, maximizes power transfer, and reduces VAR losses. In the current work, the TCSC static model is considered (shown in Fig. 1).

The line reactance of the line where the TCSC is to be located is affected by the reactance of the TCSC:

$$\mathrm{X_{LINE}} = \mathrm{x_{jk}} + \mathrm{X_{TCSC}} \tag{3}$$

$$\mathrm{X_{TCSC}} = \mathrm{K_{TCSC}} \times \mathrm{X_{LINE}} \tag{4}$$

Here 'X_{LINE}' and 'x_{jk}' is the line reactance between buses 'j' and 'k' after and before FACTS devices are placed respectively. '$\mathrm{X_{TCSC}}$' is the reactance of TCSC. 'K_{TCSC}' is the compensation coefficient of TCSC. The TCSC compensation level is estimated to be between -0.7 and 0.2.

D. CAPITAL COSTS FOR TCSC

The financial shape of the system depends deeply on the equipment's capital costs. In this paper, the life of TCSC is taken 20 years. The TCSC investment cost is determined by [10]:

$$\mathrm{COST_{TCSC}} = 0.0015 \times \mathrm{Op_{FACTS}^2} - 0.713 \times \mathrm{Op_{FACTS}} + 153.75\ \$/\mathrm{kVar} \tag{5}$$

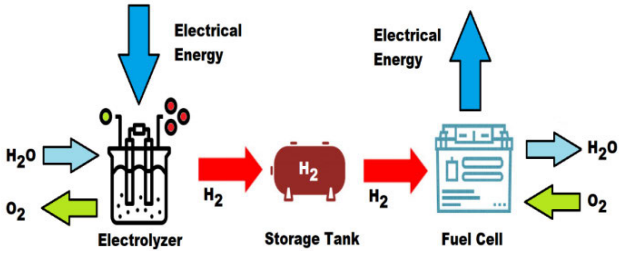

FIGURE 2. Hydrogen based fuel cell.

where, $COST_{TCSC}$ is the TCSC investment cost, Op_{FACTS} is the TCSC operating point.

E. ENERGY STORAGE SYSTEM

The hydrogen-based energy-storing device has an electrolyzer that produces hydrogen, and a fuel cell that converts the chemical energy of hydrogen into electrical energy [33].

The equation that represents the reversible chemical reaction is-

$$2\mathrm{H_2} + \mathrm{O_2} \rightarrow \mathrm{H_2O} + \text{Electrical Energy} + \text{Heat} \tag{6}$$

Tanks are used to store generated hydrogen that can be used as & when required (shown in Fig. 2). The storage system works on the following principle [34], [35]:

The Electrolyzer generates hydrogen during periods of low demand and is stored in a tank.

The energy consumed for producing hydrogen by the electrolyzer is expressed as:

$$\mathrm{E_{Elz}} = \frac{\mathrm{H2_{Elz}^{Prod}} * \mathrm{LHV_{H2}}}{\eta_{\mathrm{Elz}}} \tag{7}$$

where, $H2_{Elz}^{prod}$: Produced Hydrogen in the Electrolyzer
E_{Elz}: Energy used by the Electrolyzer
η_{Elz}: Efficiency of the Electrolyzer
LHV_{H2}: The lower heating value of hydrogen (240 MJ/kmol).

During high demand stored, Hydrogen will be used in the Fuel cell to meet the demand

During peak hours, a fuel cell can be used to generate electrical energy using hydrogen. The fuel cell's ability to produce power is directly correlated to how much hydrogen it uses.

$$\mathrm{E_{FC}} = \mathrm{H2_{FC}^{cons}} * \eta_{\mathrm{FC}} * \mathrm{LHV_{H2}} \tag{8}$$

where, $H2_{FC}^{prod}$: Hydrogen utilized by the Fuel Cell
E_{FC}: Energy generated by the Fuel cel
η_{FC}: Efficiency of the Fuel Cell
LHV_{H2}: The lower heating value of hydrogen (240 MJ/kmol).

F. RISK ASSESSMENT

In today's electricity market, risk assessment and management are becoming more and more crucial. In the area of risk management, the popular approaches are VaR and cVaR.

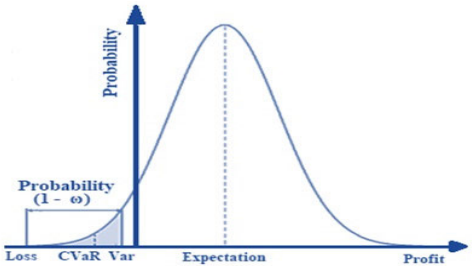

FIGURE 3. Representation of cVaR and VaR.

Based on the probabilistic investigation and guaranteed confidence levels, both estimation methods are built. For instance, cVaR might be determined using the average of the 5% worst losses if VaR is calculated at a 95% confidence level. cVaR is the extra losses in the remaining 5%. VaR indicates the smallest loss with a loss quantity of (1-ω) percentile, while cVaR displays the average loss components in the lower tail of the loss distribution (shown in Fig. 3).

Here, ω is the confidence level and $g(x,y)$ is the loss associated with the decision vector Q, to be chosen from a certain subset x of $\dot{R}$, and the random vector y in $\dot{R}$. The probability of $g(x,y)$ is denoted by $p(y)$ not exceeding a threshold ζ is then given by [9]:

$$\psi\,(\mathrm{x},\,\zeta) = \int_{\mathrm{g(x,y)}\le\zeta} \mathrm{p(y)dy} \tag{9}$$

Mathematically the assurance level based on VaR and cVaR is measured by:

$$\zeta_\omega\,(\mathrm{x}) = \min\left\{\zeta \in \dot{\mathrm{R}} : \psi\,(\mathrm{x},\,\zeta)\right\} \tag{10}$$

$$\varphi_\omega\,(\mathrm{x}) = \frac{1}{1-\omega}\left[\left(\sum\nolimits_{\mathrm{j}=1}^{\mathrm{j}_\omega} \mathrm{p_j} - \omega\right)\mathrm{a}_{\mathrm{j}_\omega} + \sum\nolimits_{\mathrm{j}=\mathrm{j}_\omega}^{\mathrm{T}} \mathrm{p_j a_j}\right] \tag{11}$$

where T is the number of trials composed under numerous conditions and loss points are ordered as $a_1 < a_2 < a_3 \ldots\ldots < a_T$.

G. OPTIMIZATION ALGORITHMS

To address the optimal power flow problem, the nature-inspired Artificial Bee Colony algorithm (ABC) and the Moth Flame Optimization (MFO) algorithm are taken into account. Compared to the ABC algorithm, the MFO approach has stronger or superior convergence capabilities, and both ABC and MFO provide more optimal solutions than the SQP.

Artificial Bee Colony Algorithm (ABC)

A population-based search methodology called the ABC algorithm which was developed in part as a result of honeybees' clever behavior [36]. In this instance, there are three types of bees present in the artificial colony: employed, onlookers, and scouts. Only one bee is actively employed for each food source. In other words, the quantity of bees actively working is determined by the number of food sources nearby. A scout is formed out of the employed bee whose food source has been left by the other bees. In the algorithm, a food source's position denotes a potential solution to the optimization issue, and a food source's nectar content denotes the fitness of the solution it is linked with. The number of employed bees or onlookers in the population is equal to the number of solutions.

The main stages of the ABC algorithm are as follows-

1. Initialization stage
2. Repeat
3. Employed bees stage
4. Onlooker bees stage
5. Scout bees stage
6. Memorize the best food source so far
7. Until cycle = Maximum cycle number
8. End

Moth Flame Optimization Algorithm

A novel metaheuristic optimization technique called the MFO algorithm is focused on simulating moth activity to understand their unique night-time navigational strategies [36]. Here, a moth flies by maintaining a steady angle to the moon, which is an incredibly efficient mechanism for traveling great distances in a straight line because the moon is far from the moth. However, frequently the moths get entangled in a pointless or fatal spiral journey around artificial lights. This is because the light is very close, hence keeping the same angle to the light source enables the moths to fly in a spiral pattern. To conduct optimization, the MFO method simulates this behavior mathematically.

The main stages of the MFO algorithm are-

1. Initialization stage
2. Repeat
3. Determination of error for each moth
4. Sort & assign a flame
5. Determination of the distance between flame & moth
6. Memorize the best moth position
7. Until cycle = Maximum cycle number

III. OBJECTIVE FUNCTION

Considering a test system with 'N_B' buses, 'N_{TL}' transmission lines, 'N_D' demands, and 'N_G' generators. The goal of this work is to place TCSC and fuel cells optimally in a renewable integrated deregulated system to optimize societal welfare and profit by minimizing the cost of generation and improving system risk in the presence of imbalance costs. Any performance analysis of an integrated renewable power system must account for imbalance costs. The positive imbalance cost provides greater system profit, whereas the negative imbalance cost generates lower profit, which is a result due to the simultaneous application of rewards and penalties to GENCOs by the system operators. The two objective functions used in this study are maximizing and minimizing problems respectively. The followings are the objective functions:

First component of the objective function:

$$\mathrm{Max.P_n(t)} = \mathrm{TR_n(t)} + \mathrm{IC_n(t)} - \mathrm{TGC_n(t)} \tag{12}$$

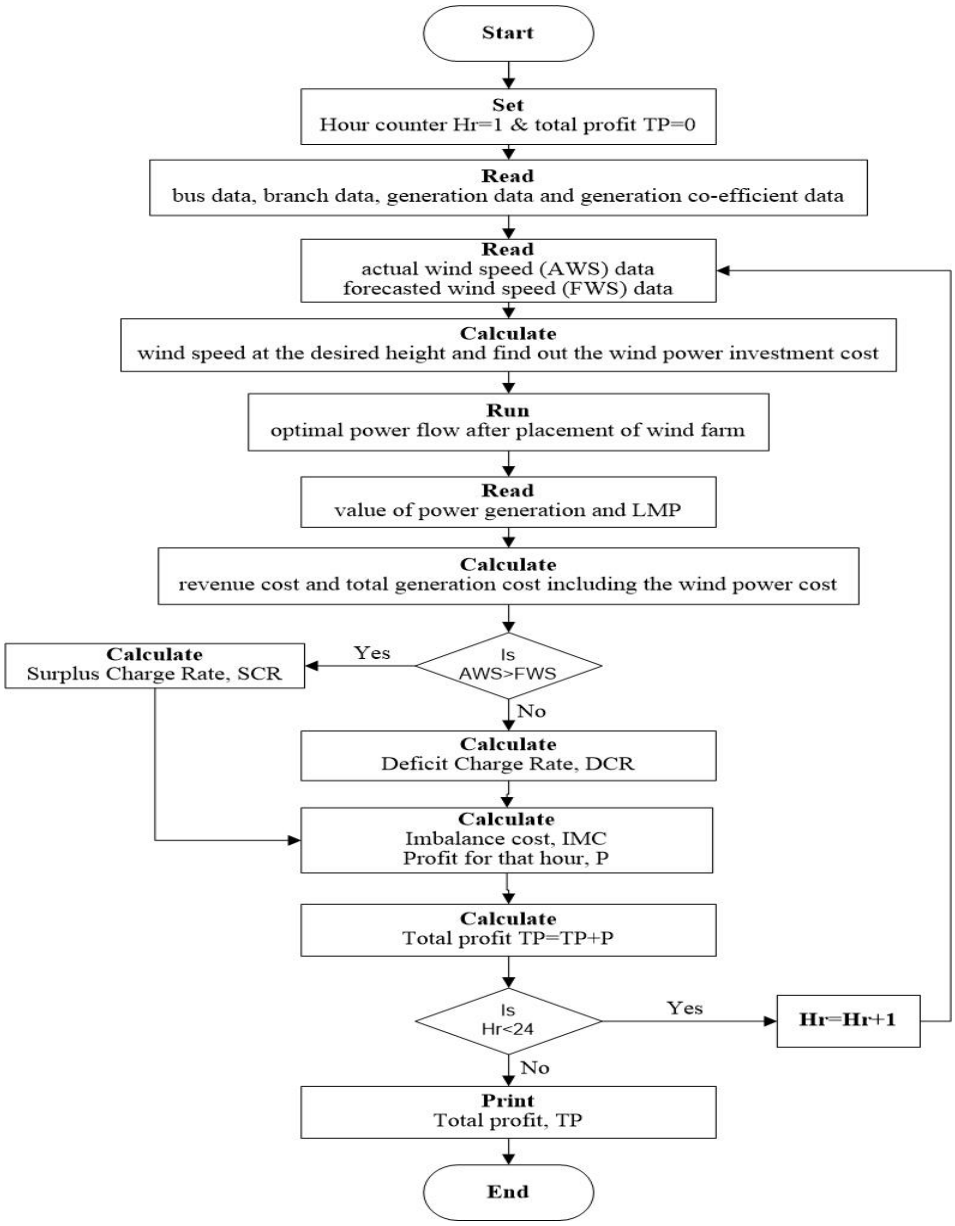

FIGURE 4. Flow chart for calculating profit.

where, $P_n(t)$ is the n-th unit's total profit at a time 't,' $TR_n(t)$ is the n-th unit's total revenue, $IC_n(t)$ is n-th unit's imbalance cost and $TGC_n(t)$ is the n-th unit's total cost (for both thermal & wind generation). This is the maximizing problem. The three components of equation (12) are system revenue, imbalance cost, and generating cost. The cost of imbalance is crucial in a deregulated energy market consisting of wind-thermal power plants to get enhanced social welfare.

$$\mathrm{TR_n(t)} = \sum_{i=1}^{N_G} \mathrm{P_{Ai}(t)} \cdot \mathrm{LMP_i(t)} \tag{13}$$

$$\mathrm{IC_n(t)} = \sum_{i=1}^{N_G} \left(\mathrm{SR(t)} + \mathrm{DR(t)} \cdot \left(\frac{\mathrm{P_{Fi}(t)}}{\mathrm{P_{Ai}(t)}} \right)^2 \right) \cdot \left(\mathrm{P_{Ai}\,(t)} - \mathrm{P_{Fi}(t)} \right) \tag{14}$$

$$\mathrm{TGC_n\,(t)} = \mathrm{GC_n\,(t)} + \mathrm{WGC_n\,(t)} + \mathrm{COST_{TCSC}} \tag{15}$$

where, $P_{Ai}(t)$ and $P_{Fi}(t)$ are power generated at i-th generator bus with actual and forecasted wind speeds. $SR(t)$ and $DR(t)$ are surplus and deficit charge rates at a time 't'. $WGC_n\,(t)$ is wind power generation cost. $GC_n\,(t)$ is the generation cost of power from a thermal generating unit and $COST_{TCSC}$ is the investment cost of TCSC devices. The system generation cost is calculated by:

$$\mathrm{GC_n\,(t)} = \sum_{i=1}^{N_G} \left(\mathrm{a_n} + \mathrm{b_n P_{Ai}(t)} + \mathrm{C_n P_{Ai}^2(t)} \right) \tag{16}$$

where, 'a_n,' 'b_n' and 'C_n' are generation cost co-efficient. Based on the anticipated wind speed, the wind-generated

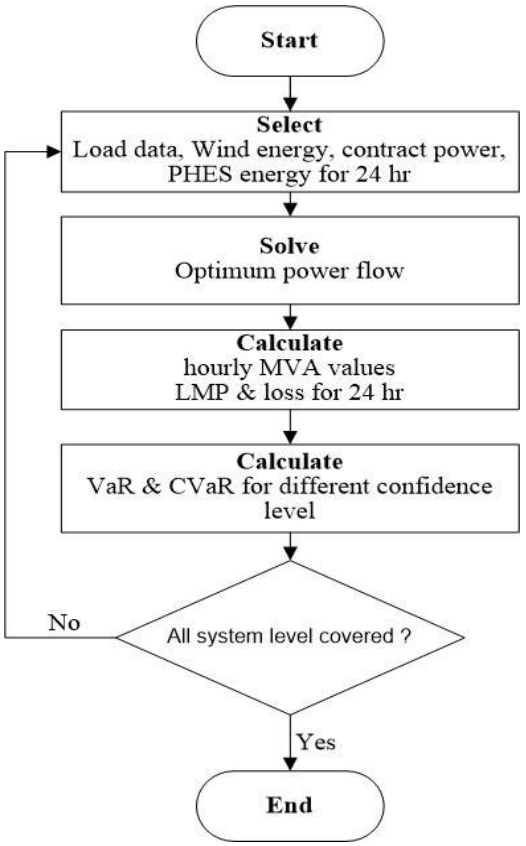

FIGURE 5. Flowchart for risk assessment.

power is calculated and committed in a day-ahead electricity market.

When AWS differs from FWS, the fuel cell can be used to reduce the power disparity and make up for the discrepancy. Equation (14) is used to calculate the cost of imbalance which is measured by the charge rate for deficit and surplus of power.

$$\mathrm{DR(t)} = (1+\lambda)\cdot \mathrm{LMP_i\,(t)}\,, \quad \mathrm{SR(t)} = 0 \text{ for } \mathrm{P_{Fi}(t) > P_{Ai}(t)}$$

$$\mathrm{SR(t)} = (1-\lambda)\cdot \mathrm{LMP_i\,(t)}\,, \quad \mathrm{DR(t)} = 0 \text{ for } \mathrm{P_{Fi}(t) < P_{Ai}(t)}$$

$$\mathrm{SR(t)} = \mathrm{DR(t)} = 0 \text{ for } \mathrm{P_{Fi}(t) = P_{Ai}(t)} \qquad (17\text{-}19)$$

where '$LMP_i\,(t)$' is Locational marginal pricing at i^{th} generation bus at a time 't'. 'λ' is the imbalance cost coefficient (ratio between the imbalance charge rate (surplus charge rate or deficit charge rate) and market clearing price). 'λ' varies from zero to one. Here it is taken 0.9.

Second component of the Objective Function:

$$\mathrm{Min.}\zeta_\omega\,(\mathrm{x}) = \min\left\{\zeta \in \dot{\mathrm{R}} : \psi\,(\mathrm{x},\zeta)\right\} \qquad (20)$$

$$\mathrm{Min.}\varphi_\omega\,(\mathrm{x}) = \frac{1}{1-\omega}\left[\left(\sum\nolimits_{\mathrm{j}=1}^{\mathrm{j}_\omega} \mathrm{p_j} - \omega\right)\mathrm{a_{j_\omega}} + \sum\nolimits_{\mathrm{j}=\mathrm{j}_\omega}^{\mathrm{T}} \mathrm{p_j a_j}\right] \qquad (21)$$

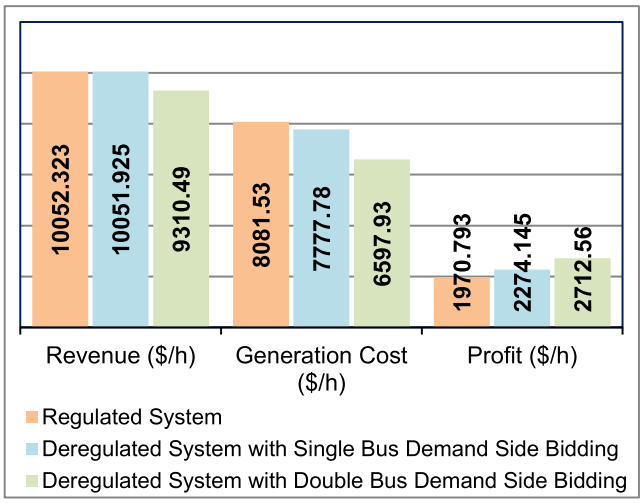

FIGURE 6. Revenue, generation cost & Profit for different systems without wind generation.

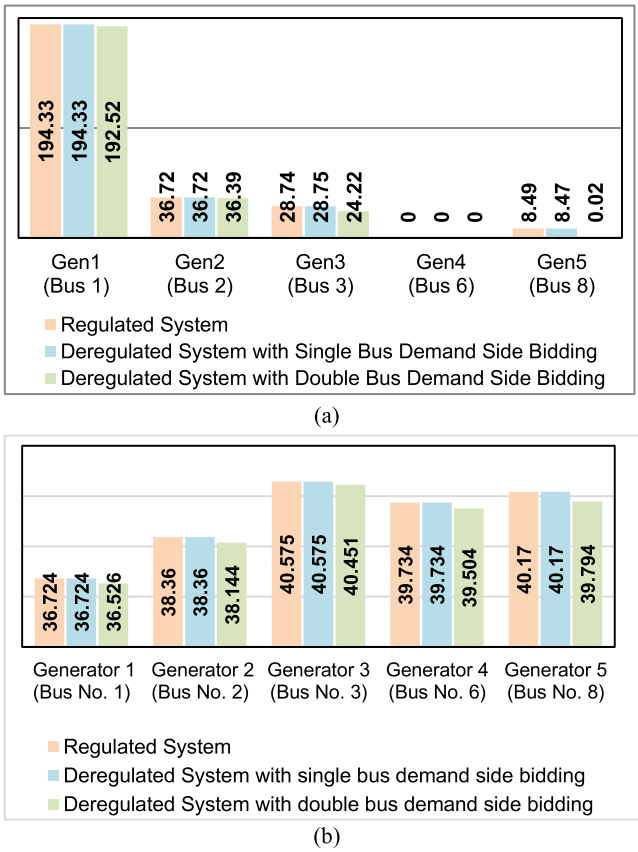

FIGURE 7. (a) Generation capacity (MW)& (b) LMP ($/MWh) at generator buses for different systems without wind generation.

Equations (20-21) respectively illustrate the functions of VaR and cVaR. VaR and cVaR have an inverse relationship with system risk, which means depending on the lowest or highest negative values of VaR and CvaR, the system risk level is at its highest or lowest. Hence risk can be reduced by moving from the left to the right tail of the system risk

TABLE 3. Comparison of bus voltage (p.u) for different systems.

Bus no.	Reg. Sys.	Dereg. Sys. with single bus DSB	Dereg. Sys. with double bus DSB	Bus no.	Reg. Sys.	Dereg. Sys. with single bus DSB	Dereg. Sys. with double bus DSB
1	1.060	1.060	1.060	8	1.060	1.060	1.060
2	1.042	1.041	1.040	9	1.047	1.044	1.060
3	1.013	1.016	1.014	10	1.042	1.039	1.052
4	1.022	1.015	1.018	11	1.047	1.046	1.053
5	1.022	1.017	1.019	12	1.045	1.045	1.046
6	1.060	1.060	1.060	13	1.040	1.040	1.042
7	1.050	1.046	1.055	14	1.026	1.024	1.034

TABLE 4. Comparison of line losses for different systems.

Line no.	Reg. Sys.	Dereg. Sys. with single bus DSB	Dereg. Sys. with double bus DSB	Line no.	Reg. Sys.	Dereg. Sys. with single bus DSB	Dereg. Sys. with double bus DSB
1	2.899	2.9	2.865	11	0.05	0.048	0.015
2	2.045	2.051	1.949	12	0.072	0.068	0.064
3	1.351	1.343	1.453	13	0.208	0.207	0.171
4	1.276	1.28	1.204	14	0	0	0
5	0.734	0.735	0.664	15	0	0	0
6	0.104	0.094	0.164	16	0.015	0.015	0.031
7	0.327	0.33	0.347	17	0.13	0.132	0.182
8	0	0	0	18	0.01	0.01	0
9	0	0	0	19	0.006	0.006	0.003
10	0	0	0	20	0.048	0.047	0.018

characteristic (shown in Fig. 3) which means VaR and cVaR value is to be increased in a positive direction. Reducing the generation cost is one of the key objectives of the current work. Now the generation cost is least when VaR and cVaR values are at the rightmost tail of the curve, indicating social welfare is maximized. Thus, social welfare and the VaR and cVaR are directly related. The solution from optimal power flow (OPF) was achieved through the different constraints which have been taken from ref. [36].

Operational constraints of Fuel Cell Energy is stored using a hydrogen storage system made up of a fuel cell, an electrolyzer, and hydrogen tanks. During off-peak hours, energy is used by the electrolyzer for the production of hydrogen molar which is stored in hydrogen tanks. The hydrogen that was saved during peak hours is utilized in a fuel cell for power production. The electrolyzer's minimum and maximum power consumption constraints are as follows [37]:

$$E_{Elz}^{Min} \leq E_{Elz} \leq E_{Elz}^{Max} \tag{22}$$

Also, the constraint for hydrogen production by electrolyzer is given by:

$$H2_{Elz}^{prod\_min} \leq H2_{Elz}^{prod} \leq H2_{Elz}^{prod\_max} \tag{23}$$

Additionally, when operating in fuel cell mode, the hydrogen that has been stored generates power to meet peak demand. Thus, the constraints are given:

$$E_{FC}^{min} \leq E_{FC} \leq E_{FC}^{max} \tag{24}$$

$$H2_{FC}^{cons\_min} \leq H2_{FC}^{cons} \leq H2_{FC}^{cons\_max} \tag{25}$$

IV. PROPOSED METHODOLOGY

This study proposes a method for assessing system risk and societal benefit in a deregulated wind-fuel cell-based electrical system. Fig. 4 and 5 represent the methodology for the system parameters improvement in terms of economy and risk respectively. The optimal economic approach calculates the profit for GENCOs based on the forecasted

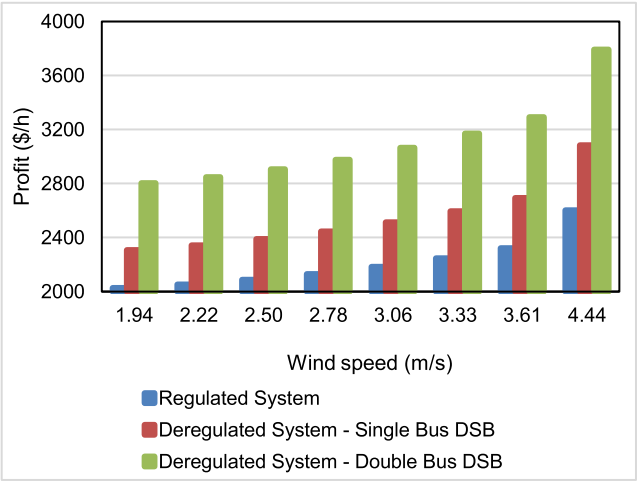

FIGURE 8. System profit vs. wind speed.

wind speed. The OPF is solved to reduce the cost of generation by rescheduling the generation and utilizing the system constraints. The imbalance cost as well as system profit is calculated once wind resources are added to the system. From the flow diagram 'H_r' represents the hour number, 'P_{Tot}' is the total profit, and 'P' is the profit for a given hour.

In Fig. 5, it is shown how to evaluate the risk and minimize it by employing fuel cells. MVA flows for each operational hour, locational marginal pricing (LMP), and system losses are gathered following each stage's solution of the optimal power flow issue. These are used to calculate cVaR and VaR while taking 95% confidence intervals into account. The system was examined throughout a 24-hour scheduling window. In this case, it is thought that the FC will help to even out the disparity between wind energy production and contractual power. Furthermore, it is believed that FC's initial capacity will be adequate to counteract any severe imbalances that may occur throughout its 24-hour operation.

TABLE 5. Revenue, generation cost for the different systems with wind generator.

Sl.	Wind speed (m/s)	Regulated System		Deregulated System with single bus DSB		Double Bus Deregulated System	
		Revenue ($/h)	Generation cost ($/h)	Revenue ($/h)	Generation cost ($/h)	Revenue ($/h)	Generation cost ($/h)
1	1.94	10,048.98	8,022.87	9,421.03	7,112.79	9,342.55	6,539.80
2	2.22	10,047.09	7,994.11	9,427.39	7,084.23	9,358.79	6,511.30
3	2.50	10,043.72	7,956.98	9,436.04	7,047.37	9,379.51	6,474.50
4	2.78	10,041.54	7,910.78	9,446.05	7,001.52	9,405.46	6,428.72
5	3.06	10,037.93	7,854.43	9,458.94	6,945.62	9,437.10	6,372.88
6	3.33	10,033.38	7,786.85	9,474.12	6,878.61	9,475.10	6,305.92
7	3.61	10,028.17	7,706.98	9,492.26	6,799.47	9,519.34	6,226.79
8	4.44	9,987.09	7,384.50	9,562.95	6,480.20	9,699.09	5,907.05

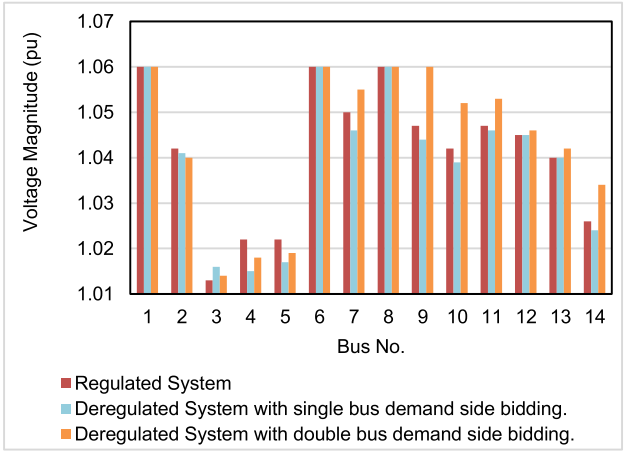

FIGURE 9. Bus voltage profile at maximum wind speed.

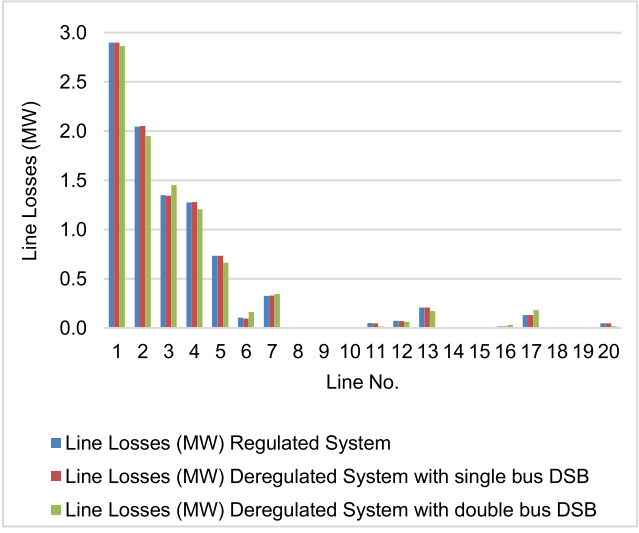

FIGURE 10. Line loss profile at maximum wind speed.

The LMP plays a vital role in the deregulated environment because LMP is the selling price of the generated power. So, minimum values of LMP can provide economic benefits to the customer which can enhance the profit of society.

TABLE 6. Hourly profit (in $/h) for Siliguri considering the imbalance cost.

Hour	FWS (m/s)	AWS (m/s)	Regulated System	Deregulated System with Single Bus DSB	Deregulated System with Double Bus DSB
1	2.22	2.50	2,090.398	2,392.290	2,906.908
2	2.22	2.50	2,090.398	2,392.290	2,906.908
3	2.22	2.50	2,090.398	2,392.290	2,906.908
4	2.22	2.22	2,049.603	2,343.154	2,847.654
5	2.22	2.22	2,049.603	2,343.154	2,847.654
6	2.22	2.22	2,049.603	2,343.154	2,847.654
7	1.94	2.22	2,052.540	2,346.120	2,848.970
8	1.94	1.94	2,020.845	2,308.238	2,802.873
9	1.94	1.94	2,020.845	2,308.238	2,802.873
10	1.94	2.22	2,052.540	2,346.120	2,848.970
11	2.22	2.22	2,049.603	2,343.154	2,847.654
12	2.22	1.94	1,960.234	2,246.865	2,777.464
13	2.50	2.78	2,137.291	2,448.858	2,979.073
14	2.50	1.94	1,882.227	2,169.555	2,744.565
15	2.50	1.94	1,882.227	2,169.555	2,744.565
16	2.50	2.22	1,971.610	2,265.859	2,814.760
17	2.22	2.50	2,090.398	2,392.290	2,906.908
18	1.94	2.50	2,092.758	2,394.668	2,908.169
19	2.22	2.78	2,140.015	2,451.550	2,980.682
20	2.22	2.22	2,049.603	2,343.154	2,847.654
21	2.22	1.94	1,960.234	2,246.865	2,777.464
22	2.22	1.94	1,960.234	2,246.865	2,777.464
23	2.22	1.94	1,960.234	2,246.865	2,777.464
24	2.22	2.22	2,049.603	2,343.154	2,847.654

V. RESULTS AND DISCUSSION

In this work, the impact of the suggested approach is examined using a modified IEEE 14-bus test system [38]. The presented approach may be performed in any small, large as well as hybrid electrical system also. The main objective of the work is to maximization of system profit which is directly linked with the minimization of system generation cost. Here, different optimization techniques have been used to get the most optimal value of generation cost by

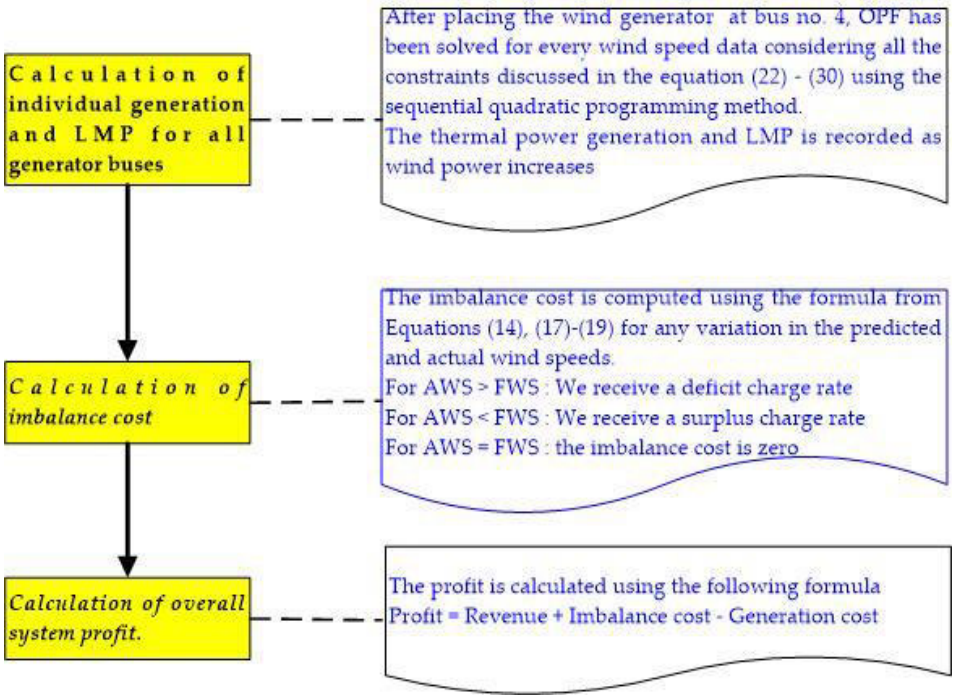

FIGURE 11. Estimation of profit considering imbalance cost.

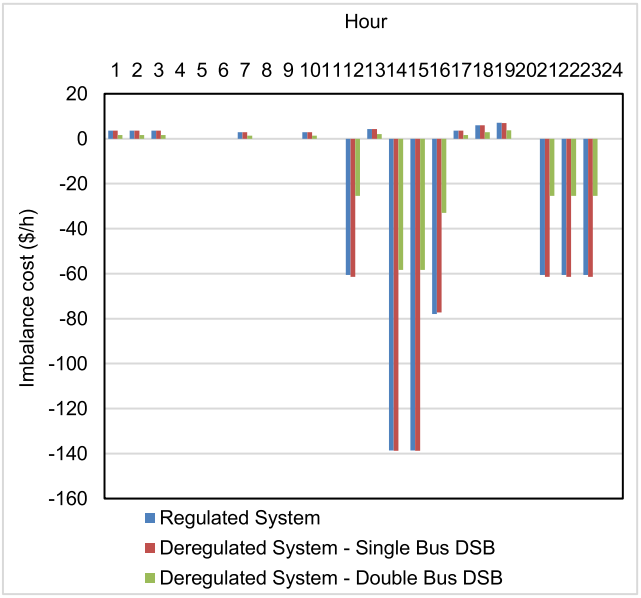

FIGURE 12. Hourly Imbalance cost (in $/h) for the considered location Siliguri.

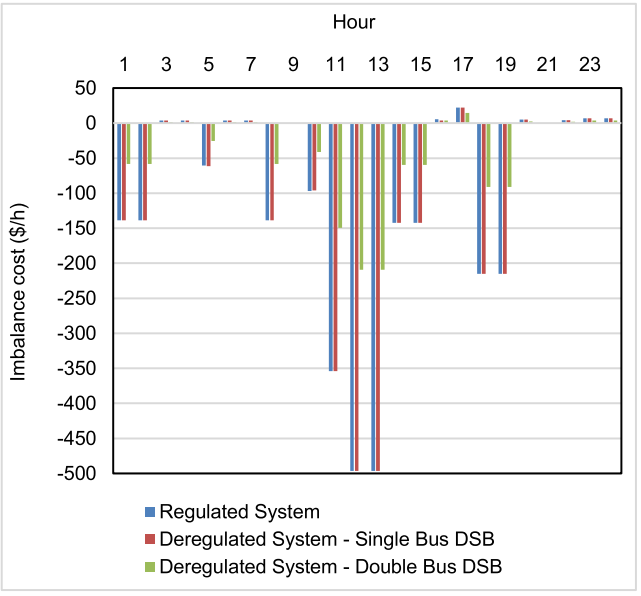

FIGURE 13. Hourly Imbalance cost (in $/h) for the considered location Kolkata.

considering different power system constraints. Similarly, the second objective of the work (i.e. system risk mitigation) also depends on the optimal power flow. The role of metaheuristic algorithms is to find the most optimal scheduling parameters after performing the optimal power flow problem. Here, three optimization techniques have been used for checking the effectiveness of the proposed approach. The OPF was initially solved using SQP, and afterward, meta-heuristic optimization techniques were applied for comparative studies.

The following scenarios have been considered during the study:

- Regulated System
- Deregulated System with single bus demand side bidding
- Deregulated System with double bus demand side bidding

Without and with the integration of wind power, the system performance under the aforementioned conditions is observed.

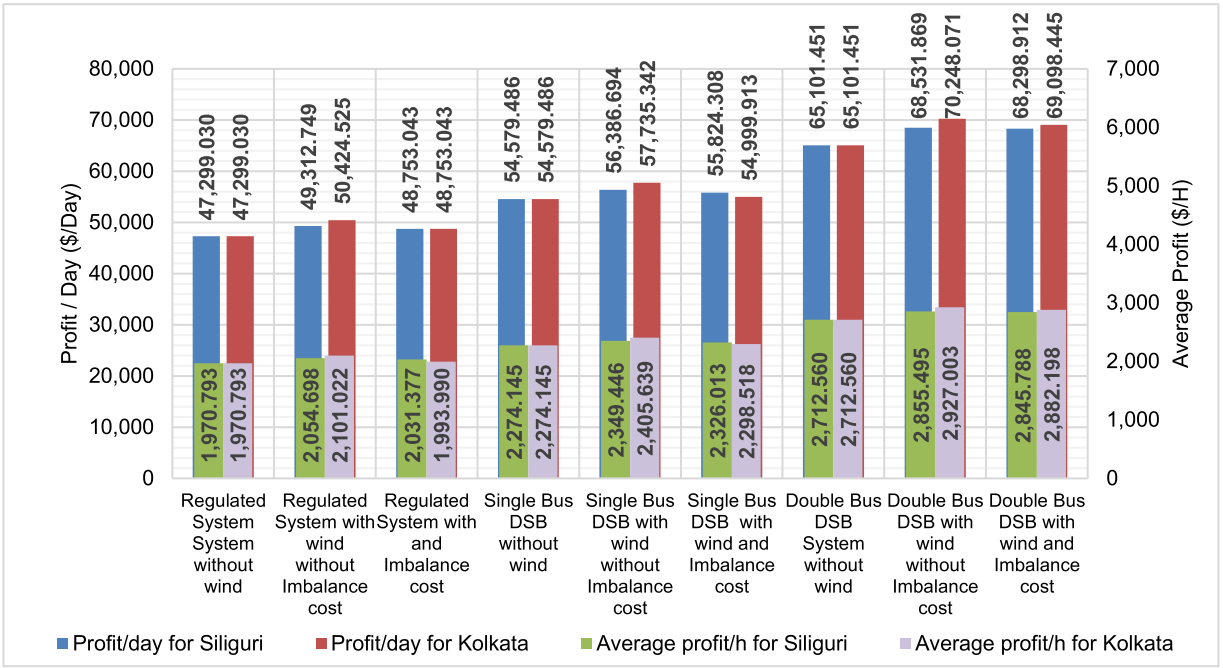

FIGURE 14. Profit/day and average profit for the selected places.

A. SYSTEM PERFORMANCE WITHOUT WIND PLACEMENT

At first, the OPF has been solved without the integration of a wind generator using SQP. Fig. 6 shows the generation cost, revenue, and profit for different considered systems. Whereas the generation capacity for all generators and LMP at the generator buses are shown in Fig. 7. Demand-side bidding has been found lower system generation costs which benefits power users directly.

The result from the demand-side bidding indicates that there is a potential for further deregulation of the current power system. Table 3 & 4 indicates a comparison of bus voltages & line losses in regulated and deregulated power systems conditions. Demand-side bidding (DSB) is conducted at bus no. 5 for single bus DSB and at buses no. 5 & 9 for double bus DSB to make the power system environment a deregulated system.

To provide flexibility bidding, both generation side and demand side bidding are considered in this work. Looking at the results shown in Fig. 7, it is observed that the cost of generation goes down and LMP improves with increasing the no. of buses for DSB. After the double demand side bidding, results show more improvement in terms of system voltage and transmission line losses. Both demand-side and generator-side bidding have succeeded in the deregulated power economy. As a result, compared to the regulated system, the power scheduling procedure has also changed. Because of the intense competition in the electricity market, customers always benefit economically. The system now contains more than one generation company, which has also enhanced the quality of the power. For these reasons, after the system was switched over to a deregulated system, improvements were noted in the bus voltage and transmission line losses.

B. SYSTEM PERFORMANCE AFTER PLACEMENT OF WIND BUT NEGLECTING IMBALANCE COST

The wind energy source is placed in bus no. 4 as this bus has the highest load connected to the system. Connecting the wind energy on this bus is going to reduce the line losses & reduce the congestion throughout the system. At first, SQP has been used to determine the optimum power flow. The overall generation cost is computed along with thermal generation and wind investment costs.

Eq. (13) has been used to compute the overall revenue cost. The revenue and generating cost for several systems with various considered wind speeds are compared in Table 5. As the system moves closer to deregulation, a decrease in total generation costs and an increase in profit may obtain. The comparison analysis of system profit with various wind speeds is shown in Fig. 8.

It has been shown that adding the most wind power to the system results in the most profit for both regulated and deregulated environments. Augmentation is evident in bus voltage and line losses after the introduction of wind power in deregulated electricity networks. Fig. 9 shows the bus voltages when the integrated wind power is maximum (at a wind speed of 4.44 m/s). Fig. 10 shows the line losses for the same condition. The cost of system generation is inversely proportional to social welfare. So, social welfare will be maximized while minimizing generation costs. In this case, including wind farms in the system results in lower generating costs, reflecting the improvement in social welfare.

C. SYSTEM PERFORMANCE WITH IMBALANCE COST

The imbalance cost offsets the effect of uncertainties of wind speed on profit. Fig. 11 describes how profit is estimated considering imbalance cost. The thermal generation & LMP

TABLE 7. Hourly profit (in $/h) for Kolkata considering imbalance cost.

Hour	FWS (m/s)	AWS (m/s)	Regulated System	Deregulated System with Single Bus DSB	Deregulated System with Double Bus DSB
1	2.22	2.50	1,887.487	2,169.555	2,744.565
2	2.22	2.50	1,882.227	2,169.555	2,744.565
3	2.22	2.50	2,090.398	2,392.290	2,906.528
4	2.22	2.22	2,090.398	2,392.290	2,906.528
5	2.22	2.22	1,960.234	2,246.865	2,777.464
6	2.22	2.22	2,090.398	2,392.290	2,906.528
7	1.94	2.22	2,090.398	2,392.290	2,906.528
8	1.94	1.94	1,882.227	2,169.555	2,744.565
9	1.94	1.94	2,086.737	2,388.667	2,905.213
10	1.94	2.22	1,989.778	2,292.470	2,864.143
11	2.22	2.22	1,667.028	1,954.356	2,653.401
12	2.22	1.94	1,524.588	1,811.916	2,593.675
13	2.50	2.78	1,524.588	1,811.916	2,593.675
14	2.50	1.94	2,047.015	2,371.045	3,004.746
15	2.50	1.94	2,047.015	2,371.045	3,004.746
16	2.50	2.22	2,342.136	2,696.666	3,296.055
17	2.22	2.50	2211.475	2535.567	3079.062
18	1.94	2.50	1,871.637	2,173.565	2,814.079
19	2.22	2.78	1,871.637	2,173.565	2,814.079
20	2.22	2.22	2,194.295	2,518.337	3,066.970
21	2.22	1.94	2,086.737	2,388.667	2,905.213
22	2.22	1.94	2,137.291	2,448.858	2,979.073
23	2.22	1.94	2,140.015	2,451.550	2,980.682
24	2.22	2.22	2,140.015	2,451.550	2,980.682

decreases as the wind power increases, resulting reduction in system generation cost. Fig. 12 and 13 display the imbalance cost for the chosen locations for 24 hours. The ISO penalizes GENCOs for failing to supply committed power, and then the imbalance cost is negative. While ISO rewards GENCOs for excess power represented by positive imbalance cost. The system profit depends on revenue cost and the cost of generation at any time. The imbalance cost and subsequently system's profit is evaluated based on the FWS & AWS. The profit values for the chosen areas are shown in Tables 6 and 7 under the regulated and deregulated electricity market scenario. To maximize the system's profit, the cost of the imbalance must be reduced. The appropriate or efficient renewable forecasting method can reduce the chances of creating an imbalance in cost for a power system.

The outcomes and conclusions drawn from the system having wind generators and taking care of the effect due to uncertainty of wind generation are summarized in Fig. 14. The comparison study for the profit while accounting for various cases for the selected locations is shown in Tables 6 & 7. The findings demonstrate that profit is maximized for every location under ''Deregulated System - Double Bus DSB with the wind without Imbalance Cost,'' while it reduces for every place with imbalance cost. Due to the unpredictable nature of wind flow, it is essential to calculate the wind speed before entering into any agreements in a deregulated power market. If there is a difference between FWS and AWS, profit may be affected; nonetheless, wind speed prediction improves the security and adaptability of the system that uses wind resources. Fig. 14 compares the daily profit for each of the chosen locations. The negative influence on profit due to imbalance cost is amply demonstrated.

In the modified IEEE 14-bus system, Fig. 14 also compares the average profit for various situations after taking imbalance costs into account. Due to the highest instances where the actual wind speed is higher than the predicted one, Kolkata was able to obtain the maximum average profit (with 2879.102 $/h) under the ''Deregulated System - Double Bus DSB with the wind with Imbalance Cost'' condition. For Siliguri, the average profit is 2845.788 dollars per hour under identical circumstances. It results from the discrepancy in wind speed predictions.

D. OPTIMAL PLACEMENT OF TCSC

All the power system constraints are taken into consideration as the optimization technique determines the best placement, cost, and minimal value of the objective function for the TCSC. The optimum location will be selected at which the objective function has the lowest value after the OPF has been run several times for every possible location for the TCSC.

Fig. 15 shows the flow chart for the optimal placement of TCSC. Where N_{TCSC} is the number of TCSC, k_{TCSC} is the compensation level of TCSC, WGC is wind generation cost, Δk_{TCSC} is an increment in k_{TCSC}, I is a variable which increases by 1 for every Δk_{TCSC} increase in TCSC compensation level, k_{TCSC}^{min} is the minimum value andk_{TCSC}^{max} is the maximum value of k_{TCSC}. In every case, OPF is solved to optimize the result. The study is carried out to judge the impacts of wind generators & TCSC in the system. Thus, each system (regulated, deregulated-single bus DSB &deregulated-double bus DSB) is investigated considering the following cases:

Case 1: System act without wind generator and TCSC.

Case 2: System act with wind generator but without TCSC.

Case 3: System act with wind generator and optimal location of TCSC.

The reactance value of the TCSC for each case is shown in Table 8 along with its optimum location. The comparative study of bus voltage & LMP for the case of a deregulated system with double DSB without & with TCSC is listed in Table 9. Fig. 16 shows the average system profit for various cases considering TCSC. It is observed that the Installation of TCSC improves the system profit for every case along with stable bus voltage.

E. SYSTEM ACT WITH THE PLACEMENT OF WIND FARM AND FUEL CELL SYSTEM

In this part, the economic evaluations that followed the integration of a Fuel Cell (FC) system into a wind-incorporated

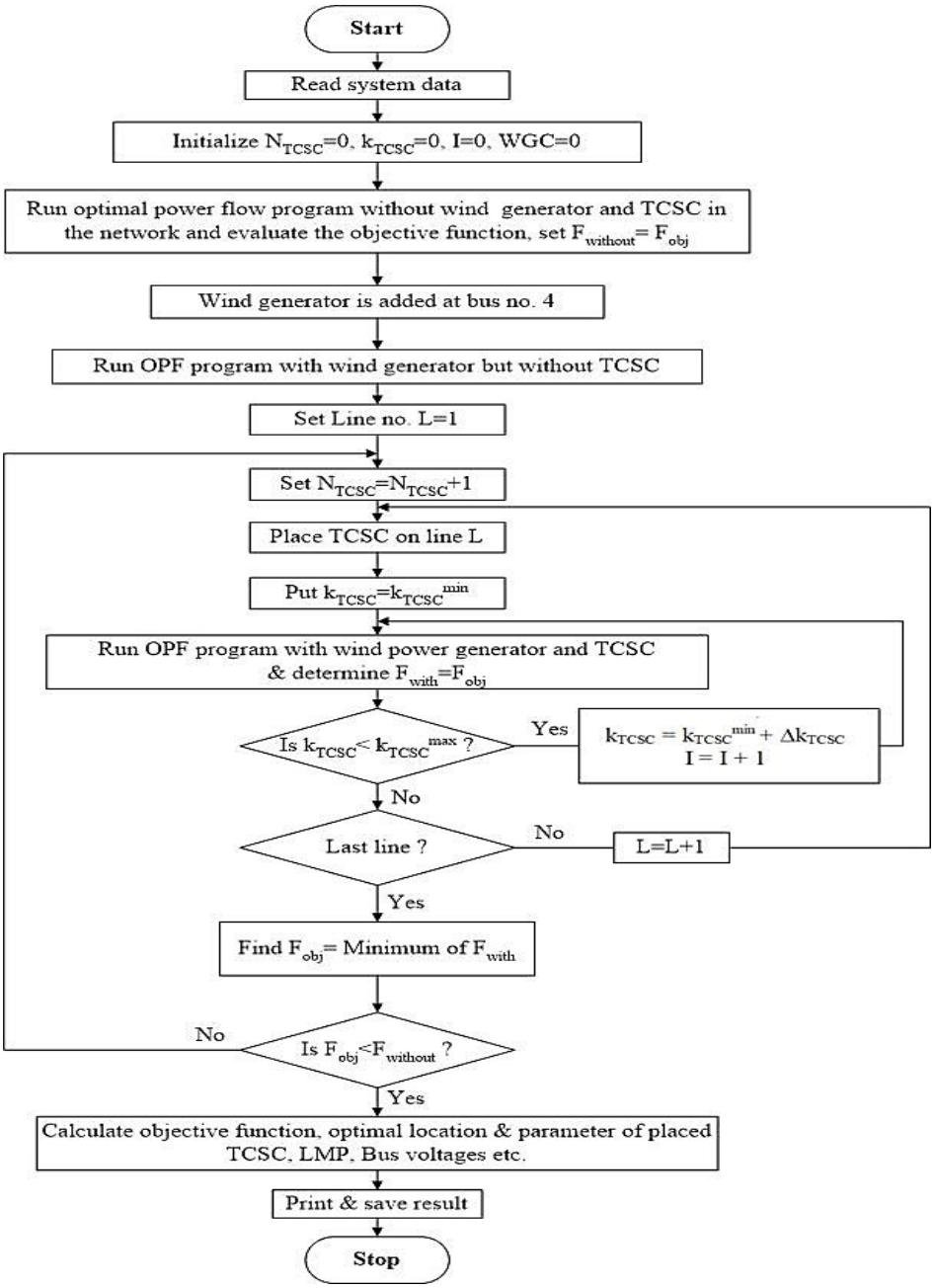

FIGURE 15. Flow-chart for optimum location of TCSC.

deregulated electrical system are provided. It is evident from the preceding section that the negative consequences of imbalance costs decrease system profit. Thus system is implemented to address this issue. When there is more wind power available and during off-peak load hours, the FC system uses an electrolyzer to make hydrogen. During other times, the FC system generates electrical energy using hydrogen. An extra amount of power is provided in this circumstance by the FC system, which will help to close the gap between the actual and predicted wind power schedules. At bus number 9, a fixed energy capacity with a 3 MW FC system has been installed. Based on the reasoning of the highest load linked to that specific bus, the bus is chosen for the FC system installation. Different optimization techniques, such as ABC and MFO, have been employed alongside SQP to test the capabilities and applicability of the given method. The MFO and ABC algorithms' parameters were taken from [36]. The average hourly profit using various optimization strategies for Siliguri and Kolkata is shown in Fig. 17.

According to the findings, establishing a wind farm with an FC system resulted in better system profitability than doing so without one. The primary innovation of this work is the application of the MFO & ABC optimization technique to a wind farm-FC hybrid system to mitigate the imbalance of

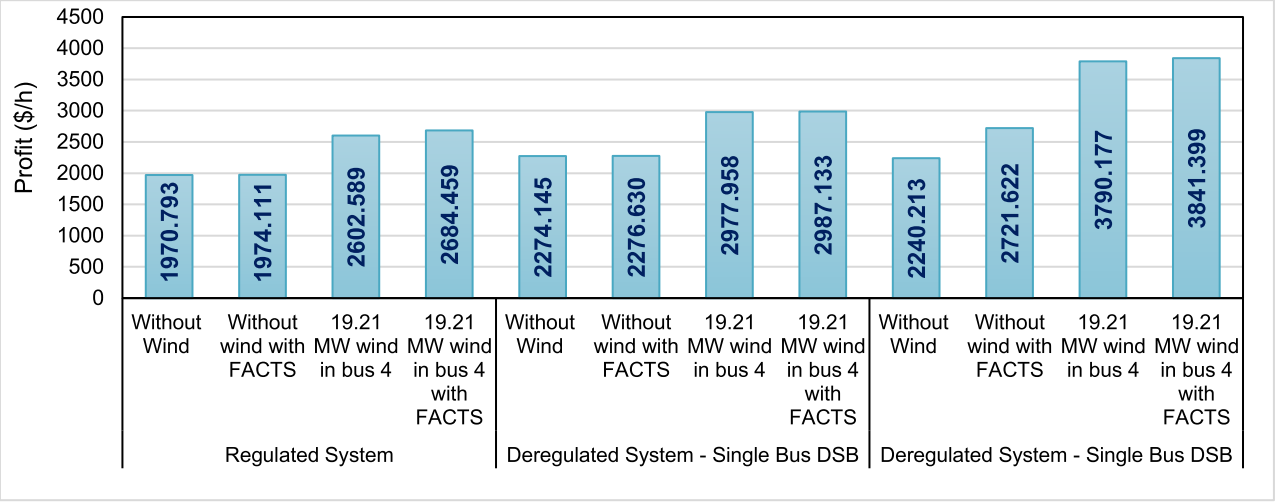

FIGURE 16. Profit comparisonfor the selected places for different conditions.

TABLE 8. Optimal location of TCSC.

System	Optimal location of TCSC at Line No	Optimal Value of TCSC
Regulated System without wind generation	2	-0.10
Regulated System with wind generation	3	-0.25
Deregulated System-Single Bus DSB Without wind generation	4	0.20
Deregulated System-Single Bus DSB With wind generation	3	-0.25
Deregulated System-Double Bus DSB Without wind generation	1	0.20
Deregulated System-Double Bus DSB With wind generation	3	-0.25

TABLE 9. Bus voltage & LMP for deregulated system-double bus DSB.

Bus No.	Deregulated System-Double Bus DSB Without wind generation				Deregulated System-Double Bus DSB With wind generation			
	Bus Voltage		LMP		Bus Voltage		LMP	
	Before TCSC	After TCSC	Before TCSC	After TCSC	Before TCSC	After TCSC	Before TCSC	After TCSC
1	1.06	1.06	36.53	36.54	1.06	1.06	36.34	36.37
2	1.04	1.042	38.14	38.14	1.04	1.04	37.94	37.98
3	1.014	1.015	40.45	40.45	1.014	1.013	40.34	40.31
4	1.018	1.019	39.87	39.86	1.018	1.019	39.56	39.59
5	1.019	1.02	39.36	39.35	1.019	1.02	39.09	39.12
6	1.06	1.06	39.50	39.49	1.06	1.06	39.14	39.18
7	1.054	1.055	39.79	39.79	1.054	1.054	39.55	39.56
8	1.06	1.06	39.79	39.79	1.06	1.06	39.55	39.56
9	1.059	1.06	39.76	39.75	1.059	1.058	39.54	39.55
10	1.053	1.052	39.92	39.92	1.053	1.051	39.68	39.70
11	1.053	1.053	39.84	39.83	1.053	1.052	39.54	39.57
12	1.046	1.046	40.14	40.12	1.046	1.046	39.77	39.81
13	1.042	1.042	40.30	40.29	1.042	1.042	39.96	40.00
14	1.034	1.034	40.81	40.80	1.034	1.033	40.54	40.56

cost and diminish the system risk. In terms of system profit maximization, MFO outperforms the other two optimization algorithms for all the considered scenarios. As a result, the installation of the FC system and the use of MFO processes boost the system to profit in the presence of an imbalance in cost.

F. SYSTEM RISK ANALYSIS WITH THE PLACEMENT OF WIND FARM AND FC SYSTEM

System risk analysis is very crucial to the safe operation of an electrical system. If a fault has occurred in the system, it must be fixed right away to prevent system failure. Here, depending on the LMP of each bus in the system, the system risk has been computed using the risk analysis tools i.e. VaR and cVaR. Utilizing various optimization techniques, Table 10 and Fig. 18 exhibit the system risk for Kolkata under various system settings. The uncertainty of renewable energy creates more system risk which can be minimized by providing additional power to the grid. After detailed studies of the results, it has been seen that the MFO algorithms provide the least degree of system risk when operating a large number of wind farms. Once the FC system is implemented, the system risk was significantly reduced in a deregulated setting. This is taking place because more power is being produced locally, which lessens the burden on the grid. The optimum placement of TCSC has reduced the system risk for all considered scenarios.

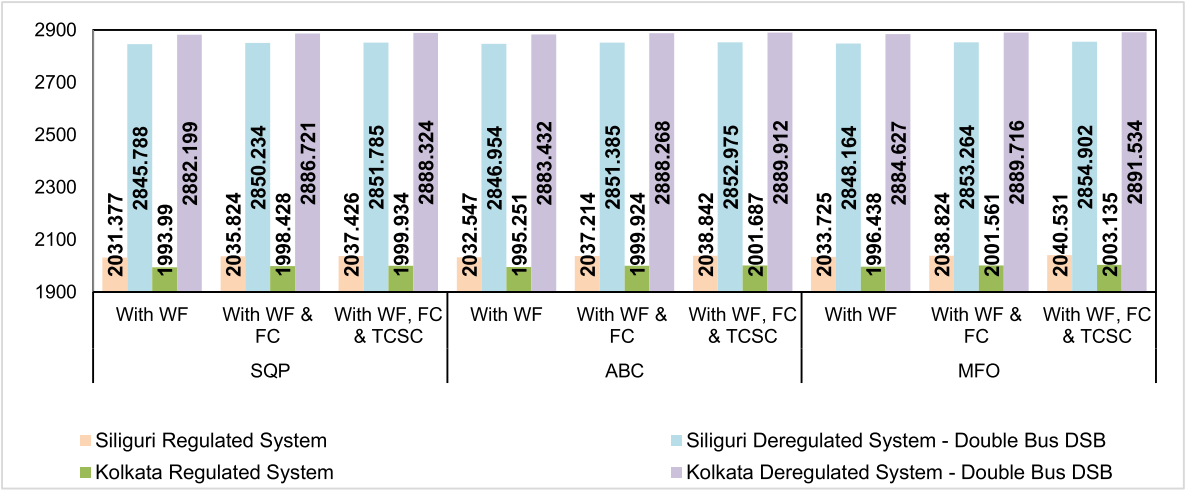

FIGURE 17. Average hourly profit with different optimization techniques for Siliguri and Kolkata.

TABLE 10. System risk with different system conditions for Kolkata with different optimization techniques.

Sl. No.	Wind Power	VaR				cVaR			
		With WF using SQP	With WF-FC - TCSC using SQP	With WF-FC - TCSC using ABC	With WF-FC - TCSC using MFO	With WF using SQP	With WF-FC - TCSC using SQP	With WF-FC - TCSC using ABC	With WF-FC - TCSC using MFO
1	19.21 MW	-0.3924	-0.3837	-0.3721	-0.3632	-0.5621	-0.5502	-0.5389	-0.5275
2	8.1 MW	-0.3624	-0.3505	-0.3401	-0.3324	-0.5428	-0.5313	-0.5201	-0.5192
3	3.42 MW	-0.3562	-0.3451	-0.3362	-0.3271	-0.5392	-0.5283	-0.5168	-0.5098

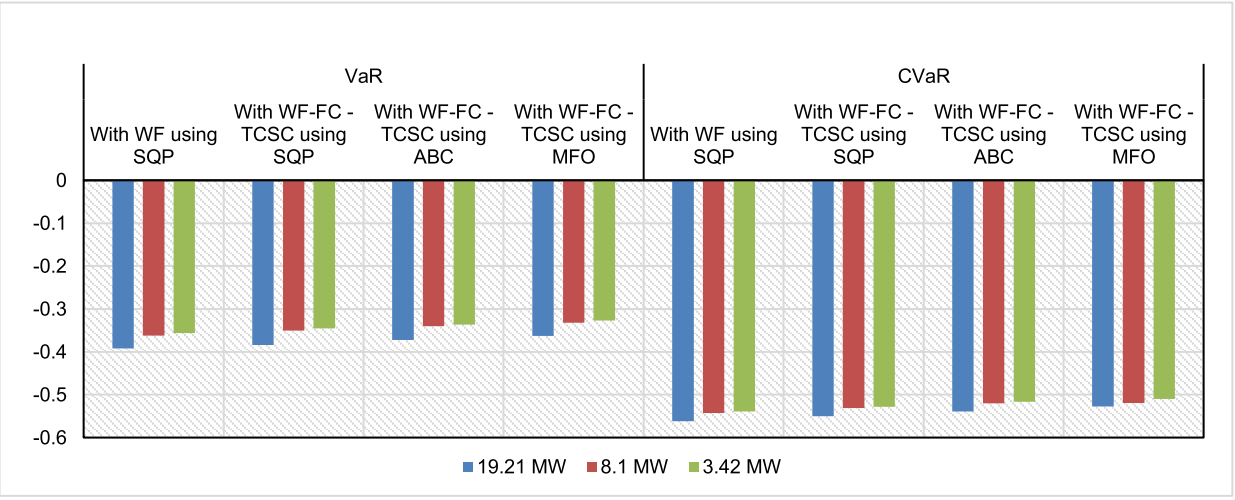

FIGURE 18. System risk with different optimization techniques for Kolkata with different system conditions.

VI. CONCLUSION

This work examines the method developed to evaluate the effects on a fuel cell – wind farm hybrid power system due to the unpredictable nature of the wind speed. It also displays how optimal placement of TCSC in the proposed system can improve the system efficiency, generation costs, voltage profiles, and electric losses in both regulated and deregulated environments. The outcome demonstrates that the suggested approach is successful in generating the highest revenues in the locations under consideration. As the GENCOs and DISCOs enter into a power supply agreement based on a wind speed estimate, any variation in actual and predicted wind speeds results deficit or excess in power delivery by the GENCOs. In such a situation the ISO may penalize or reward the GENCOs also termed the power market imbalance cost. It is observed in the study that the addition of a fuel cell

enhanced the system's LMP and hence minimized the impact of imbalance cost. The impact of the system's imbalance cost on profit is explored with the predicted and actual wind speed over a whole day for two different sites in India. The optimal power flow solution was determined, and the profit was calculated, using the ABC, MFO, and SQP optimization techniques. The use of MFO, which is the novelty of this work, performs better in terms of average yield value. The proposed hybrid system together with TCSC was also subjected to a risk analysis study in the final section employing the analysis tools (i.e., VaR and CVaR). The ABC, MFO, and SQP algorithms were used to calculate the system risk based on the LMP of each bus in the system. It has been noted that the TCSC's optimal placement lowers system risk. Regarding risk coefficient value, MFO surpasses all other optimization techniques. System risk is seen to decrease as wind generation rises. This occurs as a result of a decrease in the load demand on the grid as a result of the wind farm meeting a portion of the local load requirement.

ACKNOWLEDGMENT

This work was supported by the Researchers Supporting Project number (RSPD2023R646), King Saud University, Riyadh, Saudi Arabia. We would like to thank NIT Manipur TEQIP-III project for making available OPAL-RT Loop Simulator which helps us to validate all results of the proposed technique to detect, classify, and fault location in the grid-connected micro grid.

REFERENCES

[1] C. K. Woo, M. Kinga, A. Tishlerc, and L. C. H. Chowb, "Costs of electricity deregulation," *Energy*, vol. 31, pp. 747–768, May 2006.
[2] M. Dadashi, K. Zare, H. Seyedi, and M. Shafie-Khah, "Coordination of wind power producers with an energy storage system for the optimal participation in wholesale electricity markets," *Int. J. Electr. Power Energy Syst.*, vol. 136, Mar. 2022, Art. no. 107672.
[3] S. S. Reddy and P. R. Bijwe, "Day-ahead and real time optimal power flow considering renewable energy resources," *Int. J. Electr. Power Energy Syst.*, vol. 82, pp. 400–408, Nov. 2016.
[4] J. Matevosyan and L. Soder, "Minimization of imbalance cost trading wind power on the short-term power market," *IEEE Trans. Power Syst.*, vol. 21, no. 3, pp. 1396–1404, Aug. 2006.
[5] S. Dawn, P. K. Tiwari, and A. K. Goswami, "An approach for efficient assessment of the performance of double auction competitive power market under variable imbalance cost due to high uncertain wind penetration," *Renew. Energy*, vol. 108, pp. 230–248, Aug. 2017.
[6] G. S. Patil, A. Mulla, and T. S. Ustun, "Impact of wind farm integration on LMP in deregulated energy markets," *Sustainability*, vol. 14, no. 7, p. 4354, 2022.
[7] F. H. Gandoman, A. Ahmadi, A. M. Sharaf, P. Siano, J. Pou, B. Hredzak, and V. G. Agelidis, "Review of FACTS technologies and applications for power quality in smart grids with renewable energy systems," *Renew. Sustain. Energy Rev.*, vol. 82, pp. 502–514, Feb. 2018.
[8] S. Dawn, P. K. Tiwari, A. K. Goswami, and R. Panda, "An approach for system risk assessment and mitigation by optimal operation of wind farm & FACTS devices in centralized competitive power market," *IEEE Trans. Sustain. Energy*, vol. 10, no. 3, pp. 1054–1065, Jul. 2019.
[9] A. Das, S. Dawn, S. Gope, and T. S. Ustun, "A strategy for system risk mitigation using FACTS devices in a wind incorporated competitive power system," *Sustainability*, vol. 14, no. 13, p. 8069, Jul. 2022.
[10] P. K. Tiwari and Y. R. Sood, "An efficient approach for optimal allocation and parameters determination of TCSC with investment cost recovery under competitive power market," *IEEE Trans. Power Syst.*, vol. 28, no. 3, pp. 2475–2484, Aug. 2013.
[11] D. T. Long, T. T. Nguyen, N. A. Nguyen, and L. A. T. Nguyen, "An effective method for maximizing social welfare in electricity market via optimal TCSC installation," *Eng., Technol. Appl. Sci. Res.*, vol. 9, no. 6, pp. 4946–4955, Dec. 2019.
[12] S. Nagalakshmi and N. Kamaraj, "Secured loadability enhancement with TCSC in transmission system using computational intelligence techniques for pool and hybrid model," *Appl. Soft Comput.*, vol. 11, no. 8, pp. 4748–4756, 2011.
[13] H. Besharat and S. A. Taher, "Congestion management by determining optimal location of TCSC in deregulated power systems," *Int. J. Electr. Power Energy Syst.*, vol. 30, no. 10, pp. 563–568, 2008.
[14] V. Jayasankar, N. Kamaraj, and N. Vanaja, "Estimation of voltage stability index for power system employing artificial neural network technique and TCSC placement," *Neurocomputing*, vol. 73, nos. 16–18, pp. 3005–3011, 2010.
[15] T. Duong, J. Yao, and V. Truong, "A new method for secured optimal power flow under normal and network contingencies via optimal location of TCSC," *Int. J. Electr. Power Energy Syst.*, vol. 52, pp. 68–80, Nov. 2013.
[16] K. Sundara and H. Ravikumarb, "Selection of TCSC location for secured optimal power flow under normal and network contingencies," *Int. J. Electr. Power Energy Syst.*, vol. 34, pp. 29–37, Sep. 2012.
[17] P. P. Biswas, P. Arora, R. Mallipeddi, P. N. Suganthan, and B. K. Panigrahi, "Optimal placement and sizing of FACTS devices for optimal power flow in a wind power integrated electrical network," *Neural Comput. Appl.*, vol. 33, pp. 6753–6774, Jun. 2020.
[18] N. Acharya and N. Mithulananthan, "Influence of TCSC on congestion and spot price in electricity market with bilateral contract," *Electric Power Syst. Res.*, vol. 77, no. 8, pp. 1010–1018, 2007.
[19] A. Elmitwally and A. Eladl, "Planning of multi-type FACTS devices in restructured power systems with wind generation," *Int. J. Electr. Power Energy Syst.*, vol. 77, pp. 33–42, May 2016.
[20] K. Y. Lee, "The effect of DG using fuel cell under deregulated electricity energy markets," in *Proc. IEEE Power Eng. Soc. Gen. Meeting*, 2006, p. 8, doi: 10.1109/PES.2006.1709637.
[21] W. Smith, "The role of fuel cells in energy storage," *J. Power Sources*, vol. 86, nos. 1–2, pp. 74–83, 2000.
[22] D. Akinyele, E. Olabode, and A. Amole, "Review of fuel cell technologies and applications for sustainable microgrid systems," *Inventions*, vol. 5, no. 3, p. 42, 2020.
[23] H. Fathabadi, "Novel standalone hybrid solar/wind/fuel cell power generation system for remote areas," *Sol. Energy*, vol. 146, pp. 30–43, Apr. 2017.
[24] S. Singh, P. Chauhan, M. A. Aftab, S. S. A. I. Hussain, and T. S. Ustun, "Cost optimization of a stand-alone hybrid energy system with fuel cell and PV," *Energies*, vol. 13, p. 1295, Mar. 2020.
[25] Z. Shao, A. H. Ahangarnejad, A. Monazzah, Y. Rao, and D. Rodriguez, "Increasing of fuel cell economic benefits by optimal participation strategy with energy storages and other distributed resources and considering uncertainties and various markets," *Int. J. Hydrogen Energy*, vol. 44, no. 3, pp. 1839–1850, Jan. 2019.
[26] V. Mariani, F. Zenith, and L. Glielmo, "Operating hydrogen-based energy storage systems in wind farms for smooth power injection: A penalty fees aware model predictive control," *Energies*, vol. 15, no. 17, p. 6307, 2022.
[27] O. Utomo, M. Abeysekera, and C. E. Ugalde-Loo, "Optimal operation of a hydrogen storage and fuel cell coupled integrated energy system," *Sustainability*, vol. 13, no. 6, p. 3525, Mar. 2021.
[28] *Database: World Temperatures-Weather Around the World*. Accessed: Nov. 10, 2022. [Online]. Available: www.timeanddate.com/weather/
[29] K. M. Bataineh and D. Dalalah, "Assessment of wind energy potential for selected areas in Jordan," *Renew. Energy*, vol. 59, pp. 75–81, Nov. 2013.
[30] G. Boyle, *Renewable Energy: Power for a Sustainable Future*, 3rd ed. Oxford, U.K.: Oxford Univ. Press, 2012.
[31] P. E. Morthorst, "Costs & prices," in *Wind Energy—The Facts: 2*. The European Wind Energy Association, 2009.
[32] S. Dawn and P. K. Tiwari, "Improvement of economic profit by optimal allocation of TCSC & UPFC with wind power generators in double auction competitive power market," *Int. J. Electr. Power Energy Syst.*, vol. 80, pp. 190–201, Sep. 2016.
[33] S. Chowdhury, S. P. Chowdhury, and P. Crossley, *Microgrids and Active Distribution Networks*. London, U.K.: The Institution of Engineering and Technology, 2009.
[34] G. Cau, D. Cocco, M. Petrollese, S. K. Kær, and C. Milan, "Energy management strategy based on short-term generation scheduling for a renewable microgrid using a hydrogen storage system," *Energy Convers. Manag.*, vol. 87, pp. 820–831, Nov. 2014.

[35] S. Nojavan, K. Zare, and B. Mohammadi-Ivatloo, "Application of fuel cell and electrolyzer as hydrogen energy storage system in energy management of electricity energy retailer in the presence of the renewable energy sources and plug-in electric vehicles," *Energy Convers. Manag.*, vol. 136, pp. 404–417, Mar. 2017.
[36] N. K. Singh, C. Koley, S. Gope, S. Dawn, and T. S. Ustun, "An economic risk analysis in wind and pumped hydro energy storage integrated power system using meta-heuristic algorithm," *Sustainability*, vol. 13, no. 24, p. 13542, Dec. 2021.
[37] R. Dufo-López, J. L. Bernal-Agustín, and J. Contreras, "Optimization of control strategies for stand-alone renewable energy systems with hydrogen storage," *Renew. Energy*, vol. 32, no. 7, pp. 1102–1126, 2007.
[38] *MATPOWER—A MATLAB Power System Simulation Package, Version 5.1*. Accessed: Nov. 10, 2022. [Online]. Available: https://matpower.org/download/

JAYANTA BHUSAN BASU received the B.E. degree from Calcutta University, Shibpur, in 1995, and the M.E. degree from Bengal Engineering and Science University, in 2006. He is currently pursuing the Ph.D. degree with Maulana Abul Kalam Azad University, West Bengal, India. His current research interests include renewable energy, energy storage, optimal power flow, and deregulated electricity markets.

SUBHOJIT DAWN received the M.Tech. degree in power and energy systems engineering and the Ph.D. degree in electrical engineering from the National Institute of Technology, Silchar, India. He is currently an Assistant Professor with the Electrical and Electronics Engineering Department, Velagapudi Ramakrishna Siddhartha Engineering College, India. His current research interests include power system economics, renewable energy integration, power system planning, congestion management, smart grids, electricity market, and energy management. He is a continuous Reviewer of many reputed international (SCI/SCIE/ESCI) journals, including *IET Renewable Power Generation*, *IET Generation, Transmission and Distribution*, *Renewable Energy* (Elsevier), and *Applied Energy* (Elsevier). He is an editorial board member of several international journals. He is an Editor of *Intelligent Techniques and Applications in Science and Technology* and *Smart and Intelligent Systems* (Springer). He is also an Associate Editor of the *Journal of Electrical Engineering and Technology* (JEET) (Springer).

PRADIP KUMAR SAHA received the B.E. degree from Calcutta University, Shibpur, in 1986, the M.Tech. degree from the Indian Institute of Technology, Kharagpur, in 1988, and the Ph.D. degree from the University of North Bengal, West Bengal, in 2007. He is currently a Professor with the Department of Electrical Engineering, Jalpaiguri Government Engineering College, West Bengal. He has published more than 60 papers in international journals and conference proceedings. His current research interests include renewable energy, energy storage, optimal power flow, and electric drives. He is a life-time Fellow of the Institute of Engineer, India, and a life-time Member of the Indian Society of Technical Education (ISTE).

MITUL RANJAN CHAKRABORTY received the B.E. degree from the Jalpaiguri Government Engineering College, University of North Bengal, Jalpaiguri, in 1996, and the M.E. degree from Bengal Engineering and Science University, in 2006. He is currently pursuing the Ph.D. degree with Maulana Abul Kalam Azad University, West Bengal, India. His current research interests include renewable energy, energy storage, optimal power flow, and deregulated electricity market.

FAISAL ALSAIF received the B.Sc. degree in electrical engineering from King Saud University, Riyadh, Saudi Arabia, in 2014, and the M.A.Sc. and Ph.D. degrees in electrical engineering from The Ohio State University, OH, USA, in 2017 and 2022, respectively. He is currently an Assistant Professor with the Department of Electrical Engineering, College of Engineering, King Saud University. His research interests include power and energy, power electronics, high voltage, smart grids, and power quality improvement.

SAGER ALSULAMY received the M.Sc. degree in electrical engineering from the University of Southern California, in 2016, where he gained interest in renewable energy and climate change. His Ph.D. research involved energy decarbonization pathways for newly built cities in Saudi Arabia. During his master's studies, he has participated in the smart grids regional demonstration project and electrical vehicle program. He is a Postgraduate Research Student. His previous experience includes working in the utility as an electrical engineer in the distribution sector, testing, and commissioning high- to medium-voltage substations, routine and type tests for different electrical network equipment, such as cables, transformers, circuit breakers, and overhead lines. Currently, his research is focused on developing low carbon transition pathways plan for a non-grid-connected case study city in Saudi Arabia.

TAHA SELIM USTUN (Member, IEEE) received the Ph.D. degree in electrical engineering from Victoria University, Melbourne, VIC, Australia. He is currently a Researcher with the Fukushima Renewable Energy Institute (FREA), National Institute of Advanced Industrial Science and Technology (AIST), where he leads the Smart Grid Cybersecurity Laboratory. Before that, he was a Faculty Member with the School of Electrical and Computer Engineering, Carnegie Mellon University, Pittsburgh, PA, USA. He has invited to run specialist courses in Africa, India, and China. He has delivered talks for the Qatar Foundation, the World Energy Council, the Waterloo Global Science Initiative, and the European Union Energy Initiative (EUEI). His research has attracted funding from prestigious programs in Japan, Australia, EU, and North America. His current research interests include power systems protection, communication in power networks, distributed generation, microgrids, electric-vehicle integration, and cybersecurity in smart grids. He is a member of the IEC Renewable Energy Management WG8 and IEC TC 57 WG17. He serves on the editorial board for IEEE Access, IEEE Transactions on Industrial Informatics, *Energies*, *Electronics*, *Electricity*, *World Electric Vehicle Journal*, and *Information*.